VERSITA

Cent. Eur. J. Chem. • 9(6) • 2011 • 990-999
DOI: 10.2478/s11532-011-0087-6

Central European Journal of **Chemistry**

Ruthenium(II)-*bis*(4'-(4-ethynylphenyl)-2,2':6',2''-terpyridine) – A versatile synthon in supramolecular chemistry. Synthesis and characterization

Research Article

Ronald Siebert[1], Florian Schlütter[2], Andreas Winter[2], Martin Presselt[3], Helmar Görls[4], Ulrich S. Schubert[2,5*], Benjamin Dietzek[1,6**], Jürgen Popp[1,6]

[1]*Institute for Physical Chemistry, Jena Center for Soft Matter (JCSM), and Abbe Center of Photonics (ACP) Friedrich-Schiller-University Jena, 07743 Jena, Germany*

[2]*Laboratory of Organic and Macromolecular Chemistry (IOMC) and Jena Center for Soft Matter (JCSM) Friedrich-Schiller-University Jena, 07743 Jena, Germany*

[3]*Institute for Physics, Ilmenau University of Technology, 98693 Ilmenau, Germany*

[4]*Laboratory of Inorganic and Analytical Chemistry, Friedrich-Schiller-University Jena, 07743 Jena, Germany*

[5]*Dutch Polymer Institute (DPI) P.O. Box 902, 5600 AX Eindhoven, The Netherlands*

[6]*Institute of Photonic Technology (IPHT) Jena, 07745 Jena, Germany*

Received 26 May 2011; Accepted 29 June 2011

Abstract: A homoleptic ethynyl-substituted ruthenium(II)-*bis*terpyridine complex representing a versatile synthon in supramolecular chemistry was synthesized and analyzed by NMR spectroscopy, mass spectrometry and X-ray diffractometry. Furthermore, its photophysical properties were detailed by UV/Vis absorption, emission and resonance Raman spectroscopy. In order to place the results obtained in the context of the vast family of ruthenium coordination compounds, two structurally related complexes were investigated accordingly. These reference compounds bear either no or an increased chromophore in the 4`-position. The spectroscopic investigations reveal a systematic bathochromic shift of the absorption and emission maximum upon increasing chromophore size. This bathochromic shift of the steady state spectra occurs hand in hand with increasing resonance Raman intensities upon excitation of the metal-to-ligand charge-transfer transition. The latter feature is accompanied by an increased excitation delocalization over the chromophore in the 4`-position of the terpyridine. Thus, the results presented allow for a detailed investigation of the electronic effects of the ethynyl substituent on the metal-to-ligand charge-transfer states in the synthon for click reactions leading to coordination polymers.

Keywords: •

1. Introduction

Coordination polymers derived from transition metal ions and *bis*-terpyridine ligands are in the spotlight of smart-material research due to their widely tunable electronic and spectroscopic properties [1]. The tunability of the spectroscopic properties is achieved by varying the electronic structure of the terpyridine ligand or the connecting metal ion. These degrees of freedom open a doorway for potential applications of coordination polymers in the field of optoelectronic applications, *i.e.*, as in OLEDs or in polymer solar cells [2-6]. First ruthenium based coordination polymers have been synthesized in the 1990's [1]. Since then a rapidly

* *E-mail: ulrich.schubert@uni-jena.de*
** *E-mail: benjamin.dietzek@uni-jena.de*

growing variety of coordination polymers and oligomers based on transition metals and *bis*-terpyridine ligands have been reported [1,7-11]. The most common synthetic approach to coordination polymers and oligomers is polymerization of a *bis*-terpyridine in solution by adding metal salts and subsequent heating. Beside this widely used approach, several other strategies to create supramolecular architectures exist, *i.e.*, interconnecting of mononuclear terpyridine complexes by the formation of covalent bonds between substituents in the periphery of the terpyridine ligand. These approaches include, *e.g.*, the connection of small ruthenium(II)-*bis*terpyridine synthons by electrochemical polymerization [12], polycondensation [4], or Heck and Suzuki reactions [3,13,14]. It has further been demonstrated that click reactions can be utilized to this end [15]. This highly efficient and mild reaction was recently introduced as a synthetic tool in (supramolecular) polymer chemistry [16,17]. There, ethynyl-substituted terpyridines represent versatile substrates for the formation of 1*H*-1,2,3-triazoles by reaction with azide-functionalized derivatives (small organic molecules as well as macromolecules). Nevertheless, the synthesis of homoleptic mononuclear ruthenium(II)-*bis*terpyridine complexes, with side chains applicable for click reactions, presents an unsolved problem up to now. Herein the synthesis and characterization of a versatile precursor (**Ru2**, see Fig. 1) for coordination polymers to be derived by click reactions is presented. Furthermore, the synthon's photophysical properties are investigated by means of absorption and emission spectroscopy as well as resonance Raman spectroscopy. The spectroscopic results obtained are placed into context by a comparative evaluation of two reference complexes (**Ru1** and **Ru3**, see Fig. 1) bearing either no or an extended conjugated chromophore in the 4'-position of the terpyridine unit.

2. Experimental procedure

2.1. General

All chemicals were of reagent grade, purchased from commercial suppliers and used as received unless specified otherwise. The solvents were purchased from Biosolve and were dried and distilled according to standard procedures. Chromatographic separation was performed with standardized silica gel 60 (Merck); the reaction progress was controlled by thin layer chromatography (TLC) using aluminum sheets pre-coated with silica gel 60 F254 (Merck). Microwave-assisted reactions were carried out in a Biotage Initiator ExpEU (max. power: 400 W, frequency: 2.450 MHz) using closed reaction vials. During the reaction, the temperature and the pressure profiles were detected. The synthesis and characterization of **Ru1** and **Ru3** has been reported elsewhere in detail [38,49]. 4'-(4-Ethynylphenyl)-2,2':6',2''-terpyridine [22], (*E*)-4-(4-((2,5-*bis*(octyloxy)-4-styrylphenyl)ethynyl)phenyl)-2,2':6',2''-terpyridine [50] and $Ru(DMSO)_4Cl_2$ [20] were prepared according to the literature.

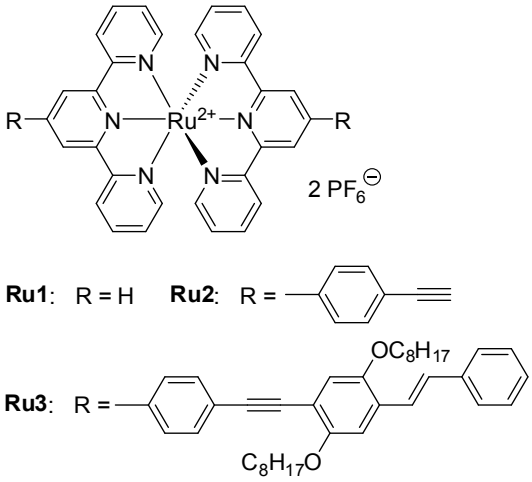

Figure 1. Molecular structure of the mononuclear ruthenium complexes (Ru1-Ru3), investigated in this contribution. Ru2 bears an ethynyl function rendering it a suitable reactant for click reactions.

2.2. Instrumentation

^{1}H NMR spectra were recorded on a Bruker AC 300 spectrometer (300 MHz) at 298 K; chemical shifts are reported in parts per million (ppm, δ scale) relative to the residual signal of the deuterated solvent; the coupling constants are given in Hz. Matrix-assisted laser desorption/ionization time-of-flight (MALDI-ToF) mass spectra were obtained from an Ultraflex III TOF/TOF mass spectrometer by dithranol as matrix in reflector and linear mode. Elemental analyses were carried out on a CHN-932 Automat Leco instrument. UV/Vis absorption spectra were measured using a UV-Vis-NIR Spectrometer (Model Varian Cary 5000), while emission spectra at 77 K were acquired using a spectrofluorimeter (Model Perkin Ellmer LS50-B). Resonance Raman spectra were measured with a conventional 90°-scattering arrangement. The lines of an argon ion laser (Model Coherent Innova 300C MotoFred Ion Laser) were used for excitation. A rotating cell was utilized to prevent heating of the samples. The scattered light was collected by a lens and focused to the slit of an Acton SpectraPro 2758i spectrometer, which was assembled with a back illuminated CCD from Princeton instruments. No changes in the absorption spectra could be observed after exposure to resonant laser light.

Ru2: A suspension of $Ru(DMSO)_4Cl_2$ (60 mg, 0.12 mmol) and 4'-(4-ethynylphenyl)-2,2':6',2''-terpyridine (83 mg; 0.24 mmol) in ethanol (15 mL) was degassed with argon for 2 hours. This mixture was heated under microwave irradiation for 2.5 hours at 105°C. After filtration and dilution with water an excess of NH_4PF_6 (150 mg) was added to precipitate the crude product. Final purification was achieved by column chromatography (silica gel, eluent: CH_3CN/H_2O/sat. aq. KNO_3 40:4:1). The combined fractions were dissolved in an ethanol/acetonitrile mixture, filtrated and an excess of NH_4PF_6 (150 mg) was added to precipitate the product. Filtration and intensive washing with water, ethanol and methanol yielded the desired complex as red powder (40 mg, 0.04 mmol, 32%). Single crystals were obtained by slow diffusion of diethyl ether into a concentrated solution of **Ru2** in CH_3CN. ^1H NMR (300 MHz, CD_3CN, 25 °C): δ = 9.01 (s, 4 H), 8.66 (d, J = 7.6 Hz, 4 H), 8.22 (d, J = 8.3 Hz, 4 H), 7.95 (t, J = 8.3 Hz, 4 H), 7.88 (d, J = 8.3 Hz, 4 H), 7.44 (d, J = 4.9 Hz, 4 H), 7.19 (t, J = 6.3 Hz, 4 H), 3.66 (s, 2 H). MALDI-ToF MS (dithranol): m/z = 913.15 [M-$(PF_6)^+$], 768.17 [M-2$(PF_6)^+$]. $C_{46}H_{30}F_{12}N_6P_2Ru$ (1057.77): calcd. C 52.53, H 2.86, N 7.95; found C 52.18, H 2.57, N 7.62.

Ru3: As reported in [38], a suspension of (*E*)-4-(4-((2,5-*bis*(octyloxy)-4-styrylphenyl)ethynyl)phenyl)-2,2':6',2''-terpyridine (76.8 mg, 0.1 mmol) and $Ru(DMSO)_4Cl_2$ (24.2 mg, 0.05 mmol) in ethanol (10 mL) was heated under microwave irradiation at 120°C for one hour. The red solution was filtered and the filtrate was treated with an excess of NH_4PF_6. After stirring at room temperature, the precipitate was filtered off. The crude product was purified by preparative size exclusion chromatography (SX-3 BioBeads™, acetone as eluent), followed by precipitation into diethyl ether to yield **Ru3** as a deep red powder (81.0 mg, 84%). ^1H NMR (d_6-acetone, 300 MHz): δ = 9.50 (s, 4H), 9.07 (d, ^3J = 8.1 Hz, 4H), 8.44 (d, ^3J = 8.3 Hz, 4H), 8.11 (m_c, 4H), 7.88 (d, ^3J = 8.6 Hz, 4H), 7.84 (d, ^3J = 6.1 Hz, 4H), 7.65–7.56 (m, 10H), 7.46 (m_c, 4H), 7.41 (m_c, 4H), 7.36 (m_c, 4H), 7.20 (s, 2H), 4.23 (t, ^3J = 6.1 Hz, 4H), 4.14 (t, ^3J = 6.6 Hz, 4H), 1.91 (m_c, 8H), 1.64 (m_c, 4H), 1.46 (m_c, 4H), 1.42–1.25 (m, 32H), 0.91 (m_c, 12H). MALDI-TOF MS (dithranol): m/z = 1871.90 ([M–PF_6]$^+$), 1726.84 (M–$(PF_6)_2$]$^+$). $C_{106}H_{114}F_{12}N_6O_4P_2Ru$ (1927.08): Calcd. C 66.07, H 5.96, N 4.36; Found C 65.81, H 6.32, N 4.68.

2.3. Crystal structure determination.

The intensity data were collected on a Nonius Kappa CCD diffractometer, using graphite-monochromated Mo-K_α radiation. Data were corrected for Lorentz and polarization effects, but not for absorption [51,52]. The structure was solved by direct methods (SHELXS) and refined by full-matrix least squares techniques against Fo^2 (SHELXL-97). Only the hydrogen atoms at *C*3 and *C*8 were included at calculated positions with fixed thermal parameters. All other hydrogen atoms were located by difference Fourier synthesis and refined isotropically [52]. XP (SIEMENS Analytical X-ray Instruments, Inc.) was used for structure representations.

2.3.1. Crystal data for Ru2.

$[C_{46}H_{30}N_6Ru]^{2+}$, 2 $[F_6P]^-$, 0.5 C_2H_3N, M_r = 1078.30 g mol^{-1}, Bordeaux-red prism, size 0.04×0.04×0.04 mm^3, triclinic, space group P$\bar{1}$, a = 9.1841(2), b = 12.5232(3), c = 19.7614(5) Å, α = 96.969(2), β = 99.435(2), γ = 92.532(1)°, V = 2220.76(9) Å^3, T= -140°C, Z = 2, $\rho_{calcd.}$ = 1.613 g cm^{-3}, μ (Mo-K_α) = 5.19 cm^{-1}, F(000) = 1082, 15004 reflections in h(-11/11), k(-16/16), l(-25/21), measured in the range 2.65° ≤ Θ ≤ 27.52°, completeness Θ_{max} = 95.6%, 9755 independent reflections, R_{int} = 0.0269, 8757 reflections with $F_o > 4\sigma(F_o)$, 665 parameters, 0 restraints, $R1_{obs}$ = 0.0518, wR^2_{obs} = 0.1275, $R1_{all}$ = 0.0603, wR^2_{all} = 0.1367, GOOF = 1.053, largest difference peak and hole: 1.101 / -1.162 e Å^{-3}.

3. Results and discussion

3.1. Synthesis and characterization.

Various methods for the preparation of ruthenium(II)-*bis*terpyridine complexes are known in the literature. In most cases, $RuCl_3 \cdot xH_2O$ is utilized for the synthesis of homoleptic (under reducing conditions in a one-step procedure) or heteroleptic species (in a directed two-step protocol) [11,18,19]. However, the comparably harsh reaction conditions often hinder the accessibility of complexes bearing (thermo)sensitive ligands. In order to overcome this limitation, Ziessel and co-workers introduced $Ru(DMSO)_4Cl_2$, as a versatile precursor complex, for the synthesis of ruthenium-*bis*tridentate complexes under relatively mild conditions [20,21]. The ethynyl moiety is a common structural motif in many terpyridine ligands with extended π-conjugated substituents (*e.g.* in so-called "molecular wires" or in arrays for artificial photosynthesis), but the homoleptic parent complex **Ru2** has not been described in the literature before.

The synthesis of **Ru2** has been carried out in moderate yield (32%) under microwave irradiation in degassed ethanol, utilizing $Ru(DMSO)_4Cl_2$ and 4'-(4-ethynylphenyl)-2,2':6',2''-terpyridine [22], as ligand. **Ru2** was characterized by ^1H NMR spectroscopy, MALDI-TOF mass spectrometry and elemental analysis (see supporting information for details). Moreover, single crystals suited for X-ray structure analysis have been

obtained, revealing the distorted octahedral geometry of the complex (Fig. 2). The structural parameters of **Ru2** (Fig. 3) have been compared to those of structurally related homoleptic complexes known from literature [23,24]: very little deviations with respect to the interligand angles and bond lengths have been observed. Furthermore, the strong deviations from a planar geometry in the ligand are directly obvious from the crystal structure, given in Fig. 2. This effect can directly be related to the steric impact between the terpyridine sphere and the ethynylphenyl moiety.

3.2. Absorption and emission spectroscopy.

Steady-state absorption spectra at room temperature as well as emission and excitation spectra at 77 K were measured to unravel the effect of the structural modifications of the terpyridine ligand. Particularly, the effect of the substituent in the 4'-position is a relevant parameter for the photophysical properties of such complexes. There are several empirical studies concerned with systematic variations of the spectroscopic parameters by varying the substitution in the 4'-position [11]. In the paper at hand, the focus is on the effect of an elongated conjugated system on the overall photophysical properties, especially on the extent of excitation delocalization over the adjacent chromophore. Such an effect has been studied on other systems before [25-27]: Some of these studies showed no effect of an elongated conjugated chromophore in the 4'-position on the absorption and emission spectra of the complexes [25,26], while other cases have been reported, in which the substitution in the 4'-position had a significant impact on the spectroscopic properties of the complexes [27]. Furthermore, it has been detailed that not only the size of the conjugated system, but also the torsional stress of the chromophore has to be taken into account because of its significant influence on the overall conjugation in the ligand system [10,28-30].

To start the discussion of the experiments presented here, Fig. 4 summarizes the absorption and emission spectra of **Ru1** – **Ru3**. Additionally, the positions of the ^{1}MLCT absorption and ^{3}MLCT emission maxima are shown. The apparent trend, *i.e.*, the absorption maxima appear bathochromically shifted upon increasing the length of the chromophore in the 4'-position, highlights the effect of the substituent on the energetic separation between S_0 and ^{1}MLCT and the respective ^{3}MLCT.

In general, the absorption spectra are dominated by intense transitions below 350 nm, assigned to ππ*-transitions of the terpyridine sphere. In **Ru1**, the pure terpyridine absorption can be observed, while for **Ru2** the ππ*-transitions of the entire conjugated system, *i.e.*, the terpyridine and the ethynylbenzene residue

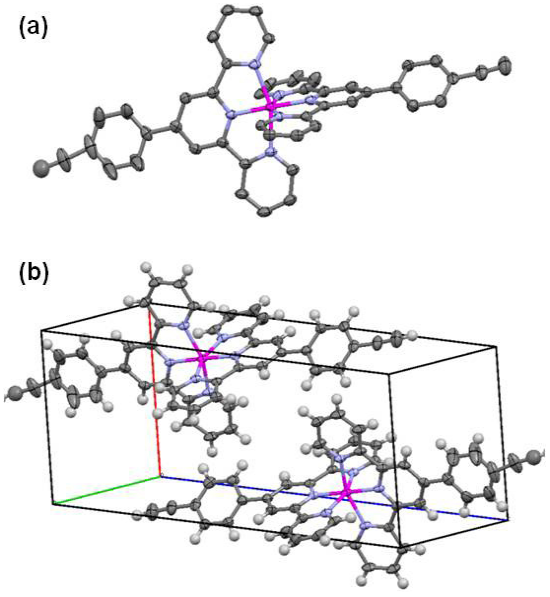

Figure 2. a) Representation of the X-ray single crystal structure of Ru2 (thermal ellipsoids at 50% probability level, hydrogen atoms omitted for clarity). (b) Elemental cell and packing of Ru2 (counterions and solvent molecules are not shown).

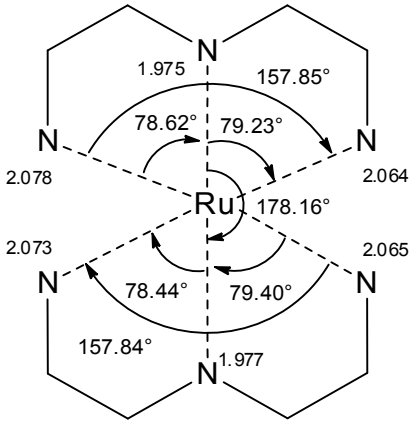

Figure 3. Selected structural parameters (bond lengths and angles) of Ru2 as determined by X-ray single crystal analysis.

contribute to the spectrum. **Ru3** reveals transitions of the entire conjugated chromophore, which are centered at about 380 nm as indicated by the isolated absorption band solely visible for **Ru3**. The bathochromic shift of this band with respect to **Ru2** arises from the increased conjugated system of the ligand. Due to the missing contribution of an adjacent chromophore in **Ru1**, the weak symmetry-forbidden dd-transitions at 350 nm are observed in this complex. As a general feature for **Ru1**–**Ru3** intense transitions appear in the visible part of the spectra, *i.e.*, at 475 (**Ru1**), 492 (**Ru2**) and 497 nm (**Ru3**). These bands, which show mutually identical vibronic fine structures due to vibrations at around 1600 cm^{-1}, are assigned to ^{1}MLCT transitions [31].

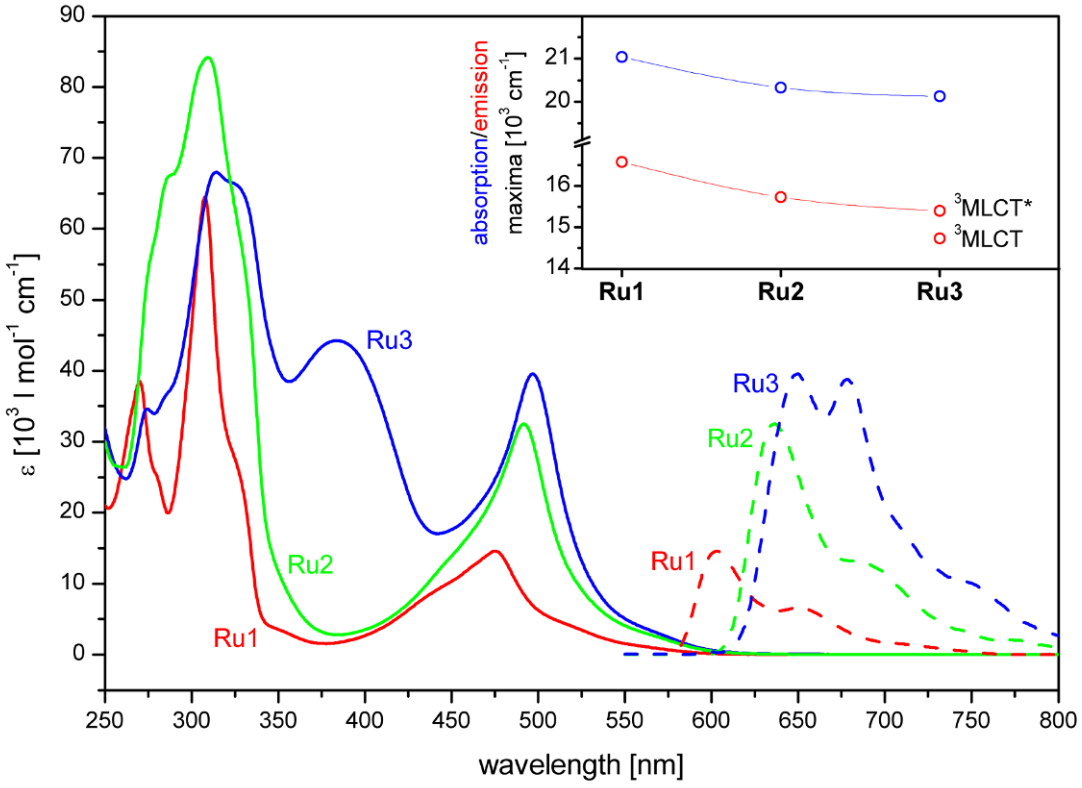

Figure 4. Room temperature absorption spectra of Ru1 (red solid line), Ru2 (green solid line) and Ru3 (blue solid line) in acetonitrile together with the emission spectra, recorded at 77 K for Ru1 (red dashed line), Ru2 (green dashed line) and Ru3 (blue dashed line). At room temperature the complexes Ru1 and Ru2 are not emissive. Furthermore, the spectral position of the ^{1}MLCT absorption maximum (blue) and the ^{3}MLCT emission maximum (red) are shown in the inset. Here, ^{3}MLCT' refers to a secondary emissive MLCT excited state in Ru3 (see main text for discussion).

The fine structure of the ^{1}MLCT transitions becomes only slightly enhanced at low temperatures (see Supporting Information). Thus, it is not possible to identify defined vibrations coupled to the electronic transition as it is possible in, *e.g.*, rigid conjugated chromophores. In the series, not only do the ^{1}MLCT absorption of **Ru1**, **Ru2** and **Ru3** shift to longer wavelengths but also the absorption cross-section increases upon increasing the size of the conjugated chromophore. Previous studies showed that the torsion angle between the terpyridine sphere and the adjacent chromophore represents a significant parameter in determining the spectroscopic features of such systems: in the electronic ground state the torsion angle is roughly 35°, while dynamic planarization of the ligand structure both in the isolated ligand and in the related transition-metal-*bis*terpyridine complexes takes place upon photoexcitation [32-35]. The 35° angle in the ground state of the complex, as obvious from the crystal structure of **Ru2**, is large enough to reduce conjugation between the terpyridine sphere and the chromophore but does not inhibit conjugation between these two molecular fragments [29,30]. Following this argumentation, the absorption spectra indicate that for **Ru2** and **Ru3** an increased excitation delocalization and, therefore, stabilization of the ^{1}MLCT should be observed. This is indicated by the bathochromic and hyperchromic shift of the ^{1}MLCT transitions compared to **Ru1**.

The emission spectra of **Ru1**–**Ru3,** recorded at 77 K, are depicted in Fig. 4. The emission is due to the radiative decay of the lowest (thermalized) ^{3}MLCT state. The emission maximum as a function of conjugated-chromophore size shows the same trend as the absorption data (inset Fig. 4). The trend also reflects the enhanced excitation delocalization in the excited state. **Ru1** and **Ru2** show similar shapes of the emission revealing an intense (v_0*-v_0)-transition at 603 (**Ru1**) and 636 nm (**Ru2**) in concert with two broad long wavelength shoulders. These are caused by vibronic progressions at around 1300 cm^{-1} – a value typical for terpyridine complexes [36,37]. Table 1 compares the spectroscopic parameters obtained from absorption and emission experiments.

The 77 K emission spectra of **Ru1** and **Ru2** reveal band shapes typical for ruthenium polypyridyl complexes [36]. On the contrary, the 77 K spectrum

Table 1. Comparison of selected spectroscopic parameters for Ru1, Ru2 and Ru3. At room temperature no emission could be detected for Ru1 and Ru2 [36].

sample	λ_{max} [nm] (absorption)	λ_{max} [nm] (emission)		emission lifetime		
		300 K	77 K	300 K [ns]	77 K [μs]	
Ru1	475.2	-	603	-	10.4 [36]	
Ru2	491.8		636		14,2	
Ru3	496.8	640 [38]	647, 677	36.5 [38]	12	214

for **Ru3** shows qualitative differences when compared to the spectra of **Ru1** and **Ru2** [38]. The emission spectrum of **Ru3** reveals two transitions of roughly equal intensity dominating the spectrum with maxima at 647 and 677 nm. These maxima are accompanied by a broad and relatively unstructured long-wavelength shoulder. This shape – atypical for ruthenium polypyridyl complexes – cannot be explained by simple vibronic progression. This is further corroborated by the emission-decay characteristics of **Ru3**, for which the emission cannot be fit by a monoexponential function. Instead the emission decays biexponentially, characterized by two lifetimes τ_1 = 12 μs and τ_2 = 214 μs (see Fig. 5). The biexponential decay of the phosphorescence shows that for **Ru3** emission does not originate from a simple radiative decay of a single ^{3}MLCT state.

One possible explanation for the luminescence properties of **Ru3** is simultaneous phosphorescence from two non-degenerate ^{3}MLCT excited states as has been observed for some ruthenium(II)-*tris*bipyridine complexes. This dual emission has – in some reports – been assigned to simultaneous emission from two distinct ^{3}MLCT states localized on different ligands in a heteroleptic complex [39,40]. However, the herein presented coordination compounds are homoleptic complexes. Therefore, such explanation cannot apply. Instead, we follow the line of arguing presented by Yersin *et al*. [41], who observed dual phosphorescence from two distinct states, termed ^{3}MLCT and ^{3}MLCT', which are associated with the same ligand structure. Thus, in **Ru3** we assign the observed emission to the ^{3}MLCT and a secondary MLCT (^{3}MLCT') state, which – due to the presence of state specific deactivation channels – are supposed to reveal different luminescence lifetimes.

3.3. Resonance Raman spectroscopy

While emission experiments can provide indications about the stabilizing effect of the conjugated chromophore in the 4'-position of the terpyridine ligand, resonance Raman (rR) spectroscopy directly yields information about the localization of the initially excited ^{1}MLCT state [42,43]. By utilizing a Raman-excitation wavelength in resonance with an electronic transition, Franck-Condon active vibrations become enhanced as compared to electronically non-resonant excitation. As these Franck-Condon active vibrations can be assigned to distinct structural features of the molecule, rR helps to identify the localization of the electronic excited state [42,44]. For recording rR spectra of **Ru1**–**Ru3**, the samples were excited in resonance with the ^{1}MLCT absorption band. It was validated that the rR intensities of Franck-Condon active vibrations, as a function of rR excitation wavelength, follow the shape of the absorption spectrum (see Supporting Information) [45,46]. Based on the agreement of the absorption spectrum and the rR intensities, the following discussion will focus on the rR spectra obtained upon excitation at 476 nm (see Fig. 6). After acquisition of the raw data, the spectra were corrected for experimental differences in the excitation power and deviations between the absorbencies at 476 nm of individual samples. The corrected rR spectra of **Ru1–Ru3** are depicted in Fig. 6 together with a non-resonant Raman spectrum of the solvent.

It is directly obvious that there are differences between the spectra of **Ru2** and **Ru1**: A number of vibrations contribute to the spectra of **Ru2**, which are absent or only very weakly visible for **Ru1** [45]. In detail, such vibrations are located at 1064 ($\delta_{ip}(py_p)$), 1254 ($\nu(py_p\text{-}py_c)$, $\delta_{ip}(py_c\text{-}H)$), 1355 ($\nu(ph\text{-}py_{trig})$) and 1532 cm^{-1} ($\delta_{ip}(py_c\text{-}ph)$). On the other hand the spectra of **Ru2** and **Ru3** are quite similar and dominantly differ only in the intensities of individual peaks. Contrary, vibrations at 1099 ($\delta_{ip}(tpy)$), 1166 ($\delta_{ip}(C_{tpy}H)$), 1473 ($\delta_{ip}(py_p)$) and 1606 cm^{-1} ($\delta_{ip}(py_c)$) appear in **Ru1**, **Ru2** and **Ru3** and get increasingly enhanced in the rR spectra taken at 476 nm with increasing chromophore size in the order **Ru1**, **Ru2**, **Ru3**. The mode assignment was done by comparison of the rR spectra with literature reports on DFT calculations and non-resonant Raman measurements on the respective ruthenium(II) and zinc(II) complexes [29,45,47].

The differences in the rR spectra can be rationalized by different localizations of the initially photoexcited ^{1}MLCT states in **Ru2** and **Ru1**. In **Ru2**, the excitation appears to be more delocalized, *i.e*., spread over the adjacent conjugated substituent at the 4'-position of the terpyridine. Consequently, Raman-active vibrations

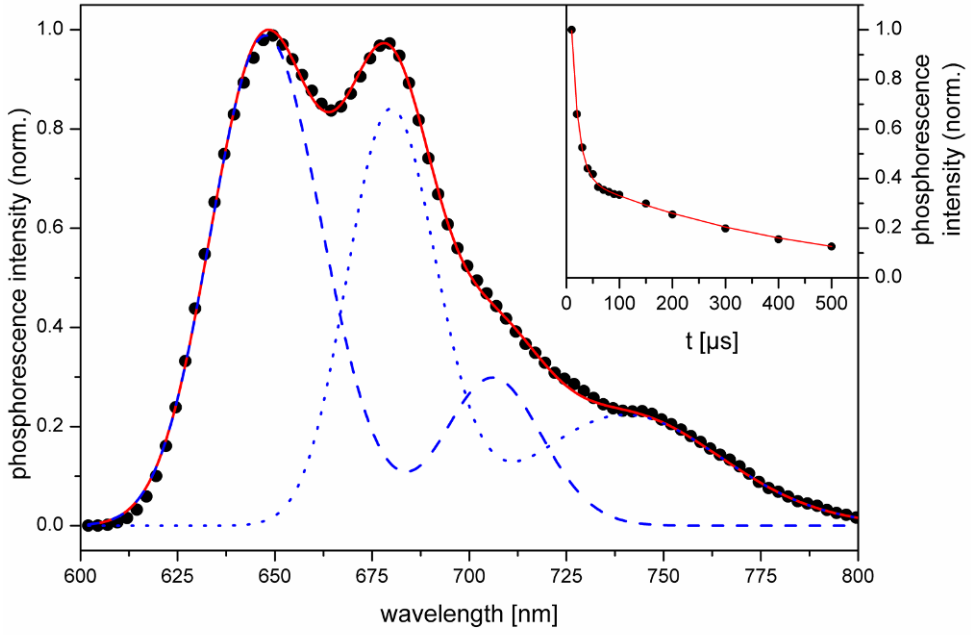

Figure 5. Deconvolution of the emission spectrum of Ru3 at 77 K (full circles) into two separate emissive species with different lifetimes of 12 μs (dashed line) and 214 μs (dotted line). The solid line refers to the resulting fit of the entire emission spectrum. The integrated emission intensity (integration between 630 and 760 nm) as a function of time is depicted in the inset of Fig. 5. The time-dependence of the emission is fit with a biexponential function.

associated with the structural elements present in **Ru2** but absent in **Ru1** become visible in the rR spectrum. However, further increase of the conjugated system from **Ru2** to **Ru3** does not lead to the appearance of vibrations in the rR spectrum, which could be assigned to direct excitation of the stilbene part of the chromophore in **Ru3**. The net effect of increasing the chromophore from **Ru2** to **Ru3** on the rR spectra is an increase of band intensities for most vibrations. This finding and the missing ν(C≡C) vibration in both **Ru2** and **Ru3** – expected at about 2200 cm^{-1} – suggest that the initial excitation is delocalized over the terpyridine sphere and the directly linked phenyl ring only. This finding is in agreement with previous theoretical studies on related systems [30,35]. A further increase of the conjugated system beyond the phenyl ring directly attached to the terpyridine causes no further delocalization of the ^{1}MLCT. However, a higher degree of conjugation between the terpyridine sphere and the adjacent phenyl ring is observed [47] causing higher rR intensities.

In previous studies on closely related zinc(II) complexes, a vibration at about 1350 cm^{-1} served as indicator for the conjugation between the terpyridine sphere and the adjacent phenyl ring. This vibration corresponds to the symmetric and asymmetric ν(ph-py(trig)) vibration [29,47]. The spectral position of this band was analyzed for the different ligand structures to deduce the effect of structural variations on the conjugation within the chromophore. For **Ru2** and **Ru3**, two vibrations are overlapping yielding the band at 1350 cm^{-1}. Therefore, the rR intensities of the ν(ph-py(trig)) vibrations are analyzed by deconvoluting the respective spectra in the region between 1320 and 1390 cm^{-1} into three Lorentz profiles [48]. The results are given in Fig. 7, which shows the original data together with the results of the fit.

From Fig. 7 it appears that the ν(ph-py(trig)) peak at 1355 cm^{-1} can be deconvoluted into two separate bands, the peak areas of which increase from **Ru2** to **Ru3** (inset Fig. 7). An altered rR intensity correlates with a change in electron density upon photoexcitation and, hence, with the localization of the electronic transition in the fraction of the molecular architecture where the molecular vibration resides. Consequently, the higher rR intensities of the 1355 cm^{-1} band is assigned to an enhanced localization of the ^{1}MLCT on the terpyridine and the adjacent phenyl ring. This structural motif is apparent in both **Ru2** and **Ru3**. The different localizations of the photoexcited states and increased rR cross sections are caused by a higher conjugation. This, in turn, causes a smaller dihedral angel between the terpyridine and the phenyl ring as predicted by theory [47]. Therefore, rR allows to obtain detailed information about the initially photoexcited ^{1}MLCT state in **Ru2**. The ethynyl-phenyl substituent causes a dramatic change in localization of the ^{1}MLCT state and hence in the rR spectrum. Thus,

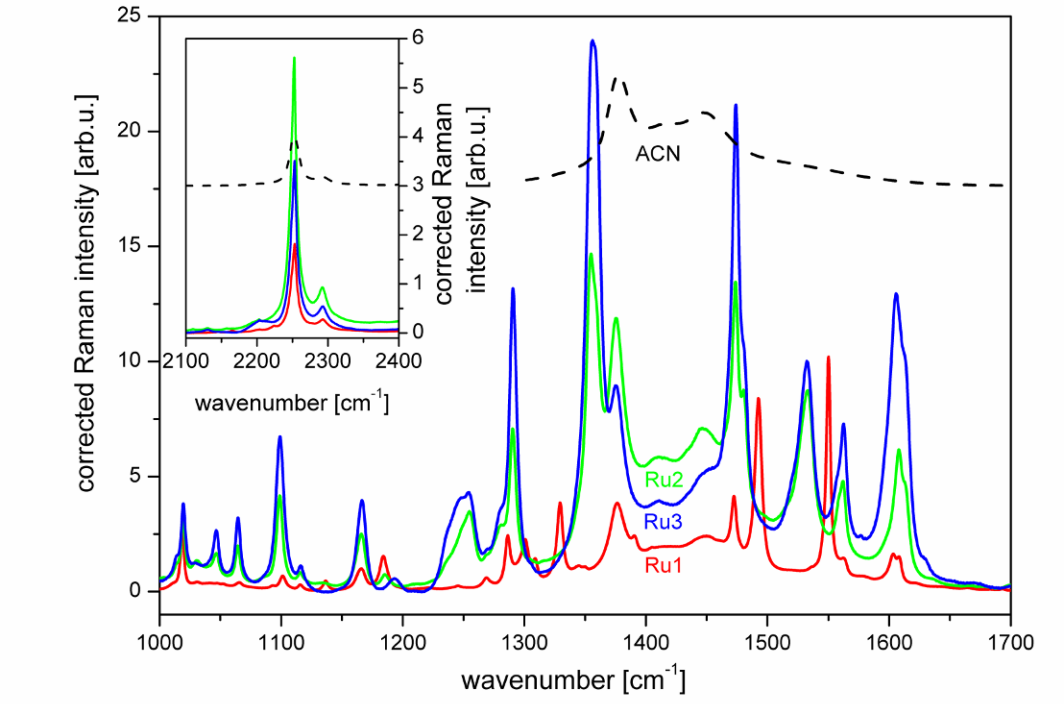

Figure 6. Resonance Raman spectra of Ru1 (red solid line), Ru2 (green solid line) and Ru3 (blue solid line) from solutions in acetonitrile (excitation at 476 nm). The non-resonant Raman spectrum of the solvent is given as reference (black dashed line, offset). The inset displays the resonance Raman spectra of Ru1–Ru3 and the nonresonant Raman spectrum of the solvent in the spectral region between 2100 and 2400 cm^{-1}. The spectral resolution of the spectrometer was approximated to 1 cm^{-1}.

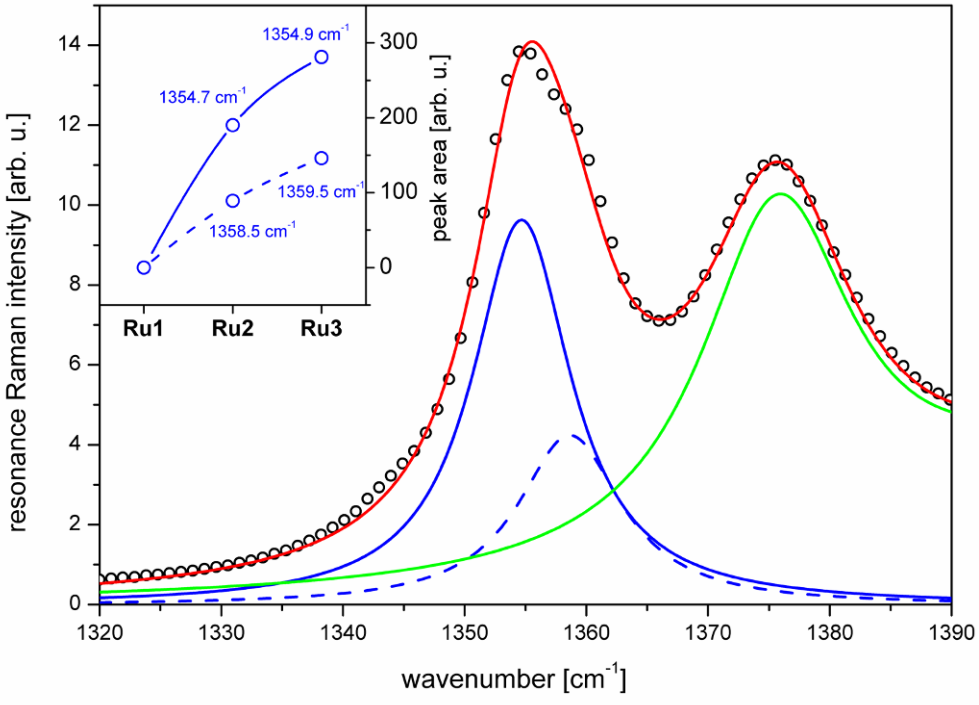

Figure 7. Fit of the resonance Raman spectra of Ru2 (circles) in the spectral region between 1320 and 1390 cm^{-1} by a sum of three Lorentz bands (red solid line). Two peaks correspond to molecular vibrations of Ru2 (blue solid and dashed line) while the solid green line represents solvent signals (acetonitrile). The inset shows the respective integrated peak areas for the series Ru1, Ru2 and Ru3.

the data show that the stabilizing effect of the ethynyl-phenyl substitution on the electronic properties of the **Ru2** is directly associated with a more delocalized photoexcited state.

4. Conclusion

A versatile synthon for supramolecular chemistry, *i.e.*, click reactions, to engineer coordination polymers, has been synthesized and spectroscopically characterized. To this extent, NMR, mass spectrometry and crystal structure determination have been performed. Due to its potential application in photoactive coordination polymers, its photophysical properties were investigated by UV/Vis absorption and emission spectroscopy as well as resonance Raman spectroscopy. The results illustrate that the conjugated substituent connected in the 4'-position has significant impact on the spectroscopic properties of the complex. This is reflected in bathochromic shifts of the absorption and emission spectra and by an increased luminescence lifetime with respect to ruthenium(II)-*bis*terpyridine. Furthermore, the delocalization of the MLCT excited states over the adjacent phenyl ring increases upon introducing the phenyl-ethynyl-substituent in the 4'-position of the ligands – a central structural motif employed in click chemistry. Further elongation of the chromophore stabilizes the ^{3}MLCT states only slightly more. However, it causes a higher conjugation in the MLCT state. A further increase of the size of the substituent in the 4'-position of the terpyridine, here a stilbene-derived chromophore was used, does not further enhance the excited-state delocalization.

References

[1] A. Wild, A. Winter, F. Schlütter, U.S. Schubert, Chem. Soc. Rev. 40, 1459 (2011)
[2] W.K. Chan, X. Gong, W.Y. Ng, Appl. Phys. Lett. 71, 2919 (1997)
[3] W.Y. Ng, W.K. Chan, Adv. Mater. 9, 716 (1991)
[4] W.Y. Ng, X. Gong, W.K. Chan, Chem. Mater. 11, 1165 (1999)
[5] P.D. Vellis, J.A. Mikroyannidis, C.N. Lo, C.S. Hsu, J. Polym. Sci., Part A: Polym. Chem. 46, 7702 (2008)
[6] A. Wild, F. Schlütter, G.M. Pavlov, C. Friebe, G. Festag, A. Winter, M.D. Hager, V. Cimrova, U.S. Schubert, Macromol. Rapid Commun. 31, 868 (2010)
[7] U.S. Schubert, C. Eschbaumer, G. Hochwimmer, Synthesis 779 (1999)
[8] V. Grosshenny, A. Harriman, R. Ziessel, Angew. Chem. Int. Ed. 34, 2705 (1995)
[9] B.G.G. Lohmeijer, U.S. Schubert, Macromol. Chem. Phys. 204, 1072 (2003)
[10] A.C. Benniston, A. Harriman, P. Li, C.A. Sams, J. Am. Chem. Soc. 127, 2553 (2005)
[11] U.S. Schubert, H. Hofmeier, G.R. Newkome, Modern Terpyridine Chemistry (Wiley-VHC, Weinheim, 2006)
[12] J. Hjelm, E.C. Constable, E. Figgemeier, A. Hagfeldt, R. Handel, C.E. Housecroft, E. Mukhtarb, E. Schofield, Chem. Commun. 284 (2002)
[13] S. Kelch, M. Rehahn, Macromolecules 32, 5818 (1999)
[14] O. Schmelz, M. Rehahn, e-Polymers 47, 1 (2002)
[15] A. Winter, A. Wild, R. Hoogenboom, M.W.M. Fijten, M.D. Hager, R.A. Fallahapour, U.S. Schubert, Synthesis 1506 (2009)
[16] D. Fournier, R. Hoogenboom, U.S. Schubert, Chem. Soc. Rev. 36, 1369 (2007)
[17] U. Mansfeld, C. Pietsch, R. Hoogenboom, C.R. Becer, U.S. Schubert, Polym. Chem. 1, 1560 (2010)
[18] H. Hofmeier, S. Schmatloch, D. Wouters, U.S. Schubert, Macromol. Chem. Phys. 204, 2197 (2003)
[19] V. Marin, E. Holder, R. Hoogenboom, U.S. Schubert, Chem. Soc. Rev. 36, 618 (2007)
[20] R. Ziessel, V. Grosshenny, M. Hissler, C. Stroh, Inorg. Chem. 43, 4262 (2004)
[21] E. Alessio, Chem. Rev. 104, 4203 (2004)
[22] A. Winter, D. A.M. Egbe, U.S. Schubert, Org. Lett. 9, 2345 (2007)
[23] D. Chartrand, I. Theobald, G.S. Hanan, Acta Crystallogr., Sect. E: Struct. Rep. Online 63, 1561 (2007)
[24] A.C. Benniston, G. Chapman, A. Harriman, M. Mehrabi, C.A. Sams, Inorg. Chem. 43, 4227 (2004)
[25] A. Harriman, A. Khatyr, R. Ziessel, A.C. Benniston, Angew. Chem. Int. Ed. 39, 4287 (2000)
[26] S. Welter, N. Salluce, A. Benetti, N. Rot, P. Belser, P. Sonar, A.C. Grimsdale, K. Müllen, M. Lutz, A.L. Spek, L. De Cola, Inorg. Chem. 44, 4706 (2005)
[27] J.S. Bair, R.G. Harrison, J. Org. Chem. 72, 6653 (2007)
[28] M. Hissler, A. El-ghayoury, A. Harriman, R. Ziessel, Angew. Chem. Int. Ed. 37, 1717 (1998)

[29] M. Presselt, B. Dietzek, M. Schmitt, J. Popp, A. Winter, M. Chiper, C. Friebe, U.S. Schubert, J. Phys. Chem. C 112, 18651 (2008)
[30] M. Preselt, B. Dietzek, M. Schmitt, S. Rau, A. Winter, M. Jäger, U.S. Schubert, J. Popp, J. Phys. Chem. A 114, 13163 (2010)
[31] A. Cannizzo, F. van Mourik, W. Gawelda, G. Zgrablic, C. Bressler, M. Chergui, Angew. Chem. Int. Ed. 45, 3174 (2006)
[32] R. Siebert, D. Akimov, M. Schmitt, A. Winter, U.S. Schubert, B. Dietzek, J. Popp, ChemPhysChem 10, 910 (2009)
[33] R. Siebert, A. Winter, U.S. Schubert, B. Dietzek, J. Popp, J. Phys. Chem. C 114, 6841 (2010)
[34] R. Siebert, A. Winter, U.S. Schubert, B. Dietzek, J. Popp, Phys. Chem. Chem. Phys. 13, 1606 (2011)
[35] R. Siebert, C. Hunger, J. Guthmuller, F. Schlütter, A. Winter, U.S. Schubert, L. González, B. Dietzek, J. Popp, J. Phys. Chem. C, 115, 12677 (2011)
[36] A. Amini, A. Harriman, A. Mayeux, Phys. Chem. Chem. Phys. 6, 1157 (2004)
[37] B. J. Coe, D.W. Thompson, C.T. Cilbertson, J.R. Schoonover, T.J. Meyer, Inorg. Chem. 34, 3385 (1995)
[38] R. Siebert, A. Winter, B. Dietzek, U.S. Schubert, J. Popp, Macromol. Rapid Commun. 31, 883 (2010)
[39] E.C. Glazer, D. Magde, Y. Tor, J. Am. Chem. Soc. 127, 4190 (2005)
[40] E.C. Glazer, D. Magde, Y. Tor, J. Am. Chem. Soc. 129, 8544 (2007)
[41] H. Yersin, E. Gallhuber, A. Vogler, H. Kunkelyt, J. Am. Chem. Soc. 105, 4155 (1983)
[42] A.B. Myers, Chem. Rev. 96, 911 (1996)
[43] M. Schwalbe, M. Karnahl, H. Görls, D. Chartrand, F. Laverdiere, G.S. Hanan, S. Tschierlei, B. Dietzek, M. Schmitt, J. Popp, J. G. Vos, S. Rau, Dalton Trans. 4012 (2009)
[44] S. Tschierlei, B. Dietzek, M. Karnahl, S. Rau, F.M. MacDonnell, M. Schmitt, J. Popp, J. Raman Spectrosc. 39, 557 (2008)
[45] P.W. Hansen, P.W. Jensen, Spectrochim. Acta. 50A, 169 (1993)
[46] R.J.H. Clark, P.C. Turtle, D.P. Strommen, B. Streusand, J. Kincaid, K. Nakamoto, Inorg. Chem. 16, 84 (1977)
[47] A. Winter, C. Friebe, M. Chiper, U.S. Schubert, M. Presselt, B. Dietzek, M. Schmitt, J. Popp, ChemPhysChem 10, 787 (2009)
[48] S. Tschierlei, M. Karnahl, M. Presselt, B. Dietzek, J. Guthmuller, L. González, M. Schmitt, S. Rau, J. Popp, Angew. Chem. Int. Ed. 49, 3981 (2010)
[49] U.S. Schubert, C. Eschbaumer, P.R. Andres, H. Hofmeier, C.H. Weidl, E. Herdtweck, E. Dulkeith, A. Morteani, N.E. Hecker, J. Feldmann, Synth. Metals 121, 1249 (2001)
[50] A. Winter, C. Friebe, M.D. Hager, U.S. Schubert, Eur. J. Org. Chem. 801 (2009)
[51] R. Hooft, COLLECT Data Collection Software (Nonius B.V., Delft, The Netheralnds, 1998)
[52] Z. Otwinowski, W. Minor, In: C.W. Carter, R.M. Sweet (Eds.), Processing of X-Ray Diffraction Data Collected in Oscillation Mode in Methods in Enzymology in Macromolecular Crystallography (Academic Press, San Diego, USA, 1997) Part A, Vol. 276, p.307